frontiers in Earth Science

ORIGINAL RESEARCH
published: 01 July 2021
doi: 10.3389/feart.2021.681931

The Reservoir Age Effect Varies With the Mobilization of Pre-Aged Organic Carbon in a High-Altitude Central Asian Catchment

*Natalie Schroeter[1], Jens Mingram[2], Julia Kalanke[2], Stefan Lauterbach[3,4], Rik Tjallingii[2], Valérie F. Schwab[1] and Gerd Gleixner[1]**

[1]Research Group Molecular Biogeochemistry, Max Planck Institute for Biogeochemistry, Jena, Germany, [2]Climate Dynamics and Landscape Evolution, Helmholtz Centre Potsdam, GFZ German Research Centre for Geosciences, Potsdam, Germany, [3]Leibniz Laboratory for Radiometric Dating and Stable Isotope Research, Kiel University, Kiel, Germany, [4]Institute of Geosciences, Kiel University, Kiel, Germany

Lake sediments provide excellent archives to study past environmental and hydrological changes at high temporal resolution. However, their utility is often restricted by chronological uncertainties due to the "reservoir age effect" (RAE), a phenomenon that results in anomalously old radiocarbon ages of total organic carbon (TOC) samples that is mainly attributed to the contribution of pre-aged carbon from aquatic organisms. Although the RAE is a well-known problem especially in high altitude lakes, detailed studies analyzing the temporal variations in the contribution of terrestrial and aquatic organic carbon (OC) on the RAE are scarce. This is partially due to the complexity of isolating individual compounds for subsequent compound-specific radiocarbon analysis (CSRA). We developed a rapid method for isolating individual short-chain (C_{16} and C_{18}) and long-chain ($>C_{24}$) saturated fatty acid methyl esters (FAMEs) by using high-pressure liquid chromatography (HPLC). Our method introduces only minor contaminations (0.50 ± 0.22 µg dead carbon on average) and requires only few injections (≤10), therefore offering clear advantages over traditional preparative gas chromatography (prep-GC). Here we show that radiocarbon values (Δ14C) of long-chain FAs, which originate from terrestrial higher plant waxes, reflect carbon from a substantially pre-aged OC reservoir, whereas the Δ14C of short-chain FAs that originate from aquatic sources were generally less pre-aged. ^{14}C ages obtained from the long-chain FAs are in closer agreement with ^{14}C ages of the corresponding bulk TOC fraction, indicating a high control of pre-aged terrestrial OC input from the catchment on TOC-derived ^{14}C ages. Variations in the age offset between terrestrial and aquatic biomarkers are related to changes in bulk sediment log(Ti/K) that reflect variations in detrital input from the catchment. Our results indicate that the chronological offset between terrestrial and aquatic OC in this high-altitude catchment is mainly driven by temporal variations in the mobilization of pre-aged OC from the catchment. In conclusion, to obtain accurate and process-specific lake sediment chronologies, attention must be given to the temporal dynamics of the RAE. Variations in the apparent ages of aquatic and terrestrial contributions to the sediment and their mass balance can substantially alter the reservoir age effect.

OPEN ACCESS

Edited by:
Francien Peterse, Utrecht University, Netherlands

Reviewed by:
Valier Galy, Woods Hole Oceanographic Institution, United States
Rienk H. Smittenberg, Stockholm University, Sweden

***Correspondence:**
Gerd Gleixner
gerd.gleixner@bgc-jena.mpg.de

Specialty section:
This article was submitted to Biogeoscience, a section of the journal Frontiers in Earth Science

Received: *17 March 2021*
Accepted: *18 June 2021*
Published: *01 July 2021*

Citation:
Schroeter N, Mingram J, Kalanke J, Lauterbach S, Tjallingii R, Schwab VF and Gleixner G (2021) The Reservoir Age Effect Varies With the Mobilization of Pre-Aged Organic Carbon in a High-Altitude Central Asian Catchment. Front. Earth Sci. 9:681931. doi: 10.3389/feart.2021.681931

Keywords: compound-specific radiocarbon analysis, leaf waxes, HPLC, XRF, reservoir age effect

INTRODUCTION

Lake sediments provide excellent high-resolution archives of regional environmental and climatic changes in the past. A prerequisite for paleoenvironmental reconstructions from lacustrine sediments are, however, reliable chronologies. Radiocarbon (^{14}C) dating has been one of the most widely used dating techniques for lake sediment records spanning the last ~50,000 years (Hughen et al., 2004; Reimer et al., 2013). Yet, ^{14}C dating of lacustrine sediments has proven to be a challenging task, since many lakes are characterized by anomalously old ^{14}C ages of sedimentary total organic material owing to a reservoir age effect (RAE, also termed "old carbon", "dead carbon" and "hard water" effect) (Hou et al., 2012; Mischke et al., 2013). The most common cause of the RAE is the dissolution of ^{14}C-depleted inorganic carbon in the lake water and its incorporation by aquatic plants and organisms (Philippsen, 2013; Zhang et al., 2016). This carbon is typically derived from the remobilization of pre-aged terrestrial OC (Howarth et al., 2013) and carbonate rocks in the catchment (Hou et al., 2012; Mischke et al., 2013). Terrestrial plant macrofossils, if deposited soon after their death, are the most suitable material for accurate ^{14}C dating, since they incorporate carbon in equilibrium with atmospheric CO_2 (Bertrand et al., 2012) and therefore do not require a reservoir effect correction. Yet, especially in arid and cold high-altitude and -latitude regions where the terrestrial vegetation cover is commonly sparse, total organic carbon (TOC) or aquatic organic matter are often the only available material that can be used for ^{14}C dating. This, however, results in large temporal and spatial uncertainties of the RAE since TOC contains a mixture of allochthonous and autochthonous carbon and therefore contributions from ^{14}C-dead or ^{14}C-depleted sources (Hou et al., 2012). As a consequence, age models for lacustrine sequences from such settings are commonly established by assessing the present-day RAE and correcting chronologies based on ^{14}C-dating of TOC or aquatic organic matter by assuming a constant RAE over time, which may be misleading (Geyh et al., 1998). Even though the RAE has been now known for over 60 years (Philippsen, 2013), detailed studies regarding the temporally variable influence of terrestrial OC and aquatic OC on the RAE are rarely conducted. A substantial part of the existing knowledge on a variable RAE magnitude has been compiled in Central Asia (Hou et al., 2012). Central Asia has been and continues to be in the focus of paleoenvironmental research using various types of archives, such as tree rings (Sheppard et al., 2004; Liang et al., 2009; Yang et al., 2014), ice cores (Yao et al., 1996; Thompson et al., 1997; Thompson et al., 2006a; Thompson et al., 2006b) and lake sediments (Mügler et al., 2010; Doberschütz et al., 2014; Lauterbach et al., 2014; Günther et al., 2016; Zhang et al., 2017). To determine temporal variations in the RAE, compound-specific radiocarbon analysis (CSRA) of individual terrestrial and aquatic biomarkers is increasingly employed, as this method overcomes the mixed ^{14}C signal of TOC dating (Smittenberg et al., 2004; Gierga et al., 2016). This can help to assess biomarker-specific transport characteristics and their residence times, thereby allowing an improved interpretation of processes that affect carbon cycling in various environmental settings (Eglinton et al., 1997; Makou et al., 2018). To date, however, only a relatively small number of studies carried out ^{14}C analysis of individual lipid biomarkers. Major progress in accelerator mass spectrometry (AMS) within the last three decades has made CSRA more feasible and greatly reduced the required sample size for obtaining reliable ^{14}C ages to <100 μg carbon (Eglinton et al., 1996; Pearson et al., 1998; Santos et al., 2007; Yokoyama et al., 2010; Ishikawa et al., 2018). For the isolation of individual compounds, preparative gas chromatography (prep-GC) is traditionally used (Eglinton et al., 1996; Kramer and Gleixner, 2006), but this time-consuming procedure often yields relatively low recovery rates (Haas et al., 2017). Conversely, high-pressure liquid chromatography (HPLC) strongly reduces the number of necessary injections required to isolate sufficient amounts of carbon (Ingalls et al., 2010; Bour et al., 2016; Schwab et al., 2019a).

Here, we present the results of extensive tests of a new method for the isolation of short- (C_{16} and C_{18} homologues) and long-chain fatty acids (FAs; C_{24}, C_{26} and C_{28} homologues) from the sediments of Lake Chatyr Kol, Kyrgyzstan, by preparative HPLC for subsequent CSRA. Our method introduces only minor contamination of extraneous carbon and can be easily adopted in future studies. By comparing ^{14}C data of terrestrial and aquatic biomarkers with an independent varve chronology (Kalanke et al., 2020), we assess the temporal variability of the RAE and ascertain the relative influence of aquatic and terrestrial OC on the ^{14}C dating of bulk sediment TOC.

STUDY AREA

Endorheic Lake Chatyr Kol (40°37'N, 75°18'E), the third largest lake in Kyrgyzstan (Thorpe et al., 2009), is located at 3,545 m above sea level in the south-western Tian Shan (**Figure 1**). The lake, which has a surface area of ~175 km^2 (Mosello, 2015), a width of ~12 km and a length of ~23 km, occupies the westernmost past of a large intra-montane basin (catchment area ~1,084 km^2), which is confined by the At Bashy Range in the north and the Torugart Range in the south. Quaternary sediments, eroded from these mountain ranges, cover the surrounding plains, which are used as pastures. Climate conditions in the Kyrgyz Tian Shan are predominantly controlled by the interaction of the Siberian High and the mid-latitude Westerlies (Aizen et al., 1997; Lauterbach et al., 2014), which results in a generally low mean annual air temperature of −0.34°C (Ilyasov et al., 2013) and lake ice cover from October to April. Precipitation is highest during the summer months due to convection and unstable atmospheric stratification (Aizen et al., 1995; Aizen et al., 2001); the average annual precipitation amounts to ~300 mm a^{-1} (Koppes et al., 2008). The prevailing cold climate at Lake Chatyr Kol promotes

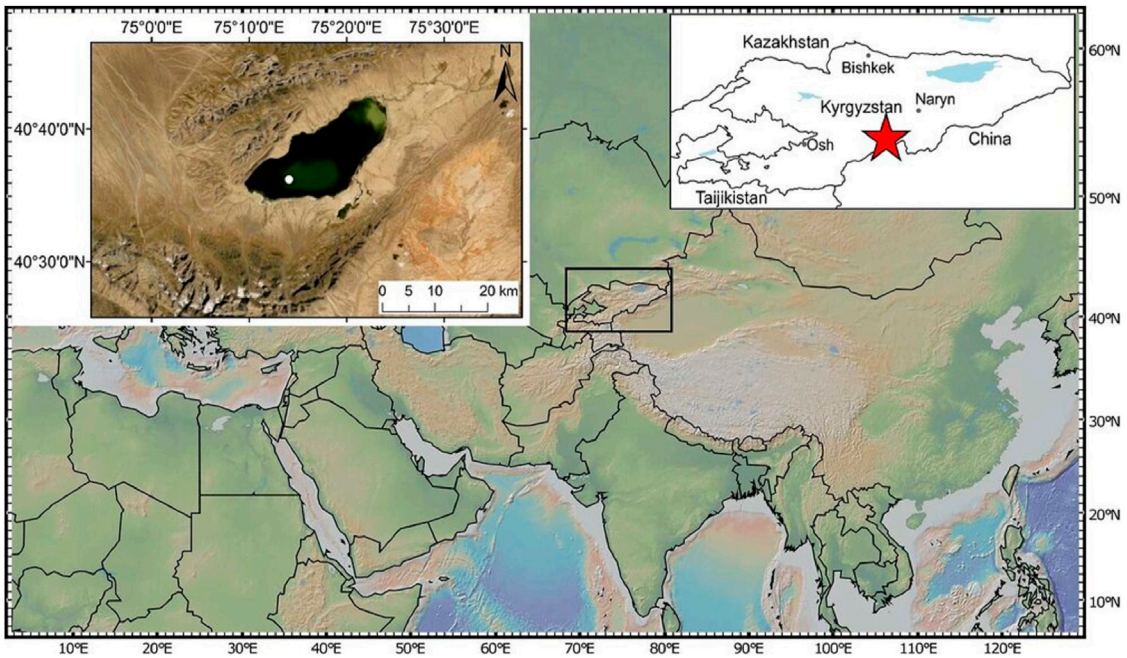

FIGURE 1 | Location of the study area. The small insert map on the right shows the location of Lake Chatyr Kol (red star) in Kyrgyzstan. The small insert map on the left shows a close-up view of the lake with the coring location (white dot). Figures made with GeoMapApp (www.geomapapp.org) and SimpleMappr (www.simplemappr.net).

the preservation of permafrost soils and widespread thermokarst formations (Shnitnikov et al., 1978; Abuduwaili et al., 2019). The sparse desert and semi-desert vegetation around the lake is dominated by montane grassland without trees (Taft et al., 2011). Due to the absence of fish stock, large numbers of the amphipod species *Gammarus alius* sp. nov., which is constrained to fresh and brackish water habitats, colonize aquatic plants (Sidorov, 2012).

MATERIALS AND METHODS

Coring and Chronology

Five sediment cores, each consisting of one or two consecutive segments of 3 m length that partially overlapped with the segments of the other cores, were recovered in July 2012 from the south-western part of Lake Chatyr Kol (40° 36.37' N, 75° 14.02' E, ~20 m water depth) by using a 60-mm-diameter UWITEC piston corer (Kalanke et al., 2020). Furthermore, six surface sediment cores were recovered in July 2012 and seven surface sediment cores were retrieved in September 2017 from different sites across the lake basin using a UWITEC gravity corer equipped with additional hammer weight (Kalanke et al., 2020). Using the piston cores recovered in 2012, a continuous composite profile (CHAT12) with a total length of 623.5 cm was compiled through correlation of the individual core segments via prominent macroscopically visible marker layers (Kalanke et al., 2020). As the sediments are annually laminated (varved) except for the uppermost 63.0 cm of the composite profile, a floating varve chronology (Chatvd19) was established by microscopic analysis of large-scale petrographic thin sections (Kalanke et al., 2020). This included the identification and characterization of different varve types, thickness measurements as well as the counting of varves. Based on the difference between two consecutive varve counts, the uncertainty of the Chatvd19 varve chronology was estimated to ~5% (Kalanke et al., 2020). In order to extend the floating varve chronology until recent times, gamma spectrometry measurements (210Pb, 137Cs) were carried out on the uppermost non-varved sediments of the CHAT12 composite profile (Kalanke et al., 2020). The measured ^{210}Pb activity concentrations were implemented in both a constant initial concentration (CIC) model (Robbins, 1978) and a constant rate of supply (CRS) model (Appleby and Oldfield, 1978). Both models are concordant with commencing elevated ^{137}Cs concentrations associated with nuclear weapon testing after AD 1945 (Pennington et al., 1973; Kudo et al., 1998; Wright et al., 1999). By extrapolating the ^{210}Pb-derived sedimentation rate, the gamma spectrometry chronology was linked at 63.0 cm composite depth to the floating varve chronology, allowing to establish a continuous age-depth model for the CHAT12 composite profile, which spans the last ~11,620 years with a mean sedimentation rate of 0.55 mm a^{-1} (Kalanke et al., 2020). The mainly varve counting-based chronology of the CHAT12 composite profile is independently confirmed by AMS ^{14}C dating of two terrestrial macrofossil samples (wood) obtained at 380.5 and 528.0 cm composite depth, which yielded conventional ^{14}C ages of 5,360 ± 40 ^{14}C a BP and 8,890 ± 50 ^{14}C a BP, respectively. These were calibrated

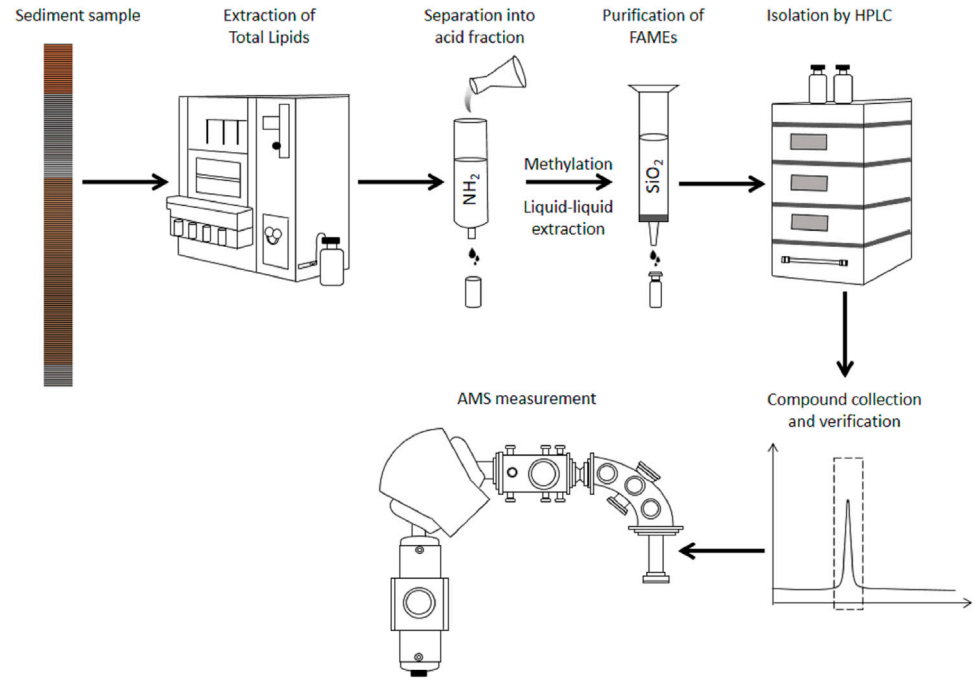

FIGURE 2 | Schematic workflow diagram of biomarker extraction, purification, isolation and CSRA.

using OxCal 4.3 (Bronk Ramsey, 1995; Bronk Ramsey, 2009) with the IntCal13 calibration data set (Reimer et al., 2013), yielding calibrated ages of 6,140 ± 137 cal. a BP and 9,988 ± 203 cal. a BP, respectively (Kalanke et al., 2020).

Since the calibrated age difference between two ^{14}C ages is not time independent, varve ages were converted to their corresponding ^{14}C ages by reading the IntCal20 calibration curve in reverse using the "uncalibrate" function of the "rcarbon" package in R4.1.0 (Crema and Bevan, 2021; R Core Team, 2021; Soulet, 2015; Soulet et al., 2016). The resulting ^{14}C age values are referred to as uncalibrated varve ^{14}C ages in the following sections. All offsets between TOC, CSRA and varve counting data are reported in ^{14}C years, accordingly.

Lipid Extraction and Purification of Fatty Acid Methyl Esters

In order to extract lipids for CSRA, ten 1-cm-thick sediment samples were taken at different depths from the CHAT12 composite profile (**Supplementary Table S1**), freeze-dried, homogenized, and subsequently processed using a pressurized solvent speed extractor (E-916, BÜCHI, Essen, Germany) with a dichloromethane/methanol mixture (9:1) at 100°C and 120 bar for 15 min in two cycles. Free fatty acids (FAs) were separated from neutral lipids, alcohols and ketones in the total lipid extract by elution with diethyl ether/acetic acid (19:1) over columns with aminopropyl-modified silica gel (CHROMABOND® NH_2 polypropylene columns, 60 Å, Macherey-Nagel, Düren, Germany). FAs were then methylated using 5% hydrochloric acid in methanol of known isotopic composition at 80°C for 12 h to yield corresponding fatty acid methyl esters (FAMEs). Subsequently, FAMEs were obtained by liquid-liquid extraction with 5% NaCl and hexane and further purified by removing other functionalized FAMEs via elution with dichloromethane over silica gel columns (~2 g). In order to minimize organic contaminants, all glassware was pre-heated to 450 °C for 5 h prior to use. A schematic overview of the workflow is depicted in **Figure 2**.

Bulk Sediment Geochemical Analyses and AMS ^{14}C Dating of Organic Material From the Lake Chatyr Kol Sediments

To assess the influence of variations in terrigenous input on the compound-specific ^{14}C ages, we analysed the major element composition of the CHAT12 sediments. These analyses were performed on the foil-covered fresh surface of the split sediment cores at 200 µm resolution using an ITRAX X-ray fluorescence (XRF) core scanner (Cox Analytical Systems, Mölndal, Sweden) equipped with a Cr X-ray tube operating at 30 kV and 30 mA. The measurement time per scanning step was 10 s. Here we only report the log-ratio of the measured intensities for potassium and titanium, reflecting relative variations of element concentrations without the potential bias of measurement and matrix effects (Weltje and Tjallingii, 2008). To better visualize the relation between the compound-specific ^{14}C ages and variations in the high-resolution XRF element data, log(K/Ti) was averaged over 1.2-cm-intervals across the positions where the individual 1-cm-thick samples for CSRA were taken.

In addition to the two pieces of wood that have been AMS ^{14}C-dated to support the Chatvd19 varve chronology (see chapter 3.1), eleven depth-matched sediments were decalcified and submitted to the Poznań Radiocarbon Laboratory, Poland, for bulk TOC AMS ^{14}C dating (Kalanke et al., 2020). The conventional ^{14}C ages are reported in **Supplementary Table S2** as well as in Kalanke et al. (2020).

Isolation of Fatty Acid Methyl Esters by High-Pressure Liquid Chromatography

Individual FAMEs were isolated using an Agilent Technologies 1,200 Series HPLC system consisting of a vacuum degasser, a quaternary pump, a thermostat-controlled column compartment, an injection autosampler, a UV detector and a fraction collector (**Figure 2**). Separation was achieved on a reverse-phase column (Nucleodur® C8 Gravity, 250 mm × 4.6 mm, 5 µm particle size, Macherey-Nagel, Düren, Germany) along with a guard column (Macherey-Nagel, Düren, Germany), using an isocratic elution with 100% acetonitrile (ACN) at a flow rate of 1.0 mL min^{-1}. The column was maintained at a constant temperature of 40°C and compounds were detected at a wavelength of 230 nm. Elution times of the short- and long-chain FAMEs and their stability have been determined beforehand by standard runs and were adjusted daily. Typical collection durations for FAMEs C16:0 to C28:0 were 20, 19, 36, 36, 40 s, respectively. Up to 10 injections of each sample with an injection volume of 10 µL were made to ensure quantities of 20—150 µg carbon required for CSRA using EA/AMS. Collected fractions of the same compounds were pooled into gas chromatography vials and evaporated to a volume of ~2 mL under a stream of ultra-high-purity N_2. In order to assure the purity of the collected FAMEs and to determine the recovery of carbon prior to ^{14}C measurements, aliquots of 5 µL of several samples were run on a gas chromatograph (GC) equipped with a flame ionization detector (GC-FID, Agilent 7890B, Agilent Technologies, Santa Clara, United States) (**Figure 2**). The identification of the individual compounds was achieved relative to a FAME standard mixture on an Ultra two column (50m, 0.32 mm ID, 0.52-µm film thickness, Agilent Technologies, Santa Clara, United States). The PTV injector was operated in splitless mode, starting at 45°C for 0.1 min and heating up to 300°C at 14.5°Cs^{-1} (hold for 3 min). The GC oven increased from 140°C (hold for 1 min) to 310°C at a rate of 4°C min^{-1} (hold for 15 min) and finally to 325°C at 30°C/min (hold for 3 min). Since the concentrations of long-chain FAMEs in the Lake Chatyr Kol sediments were relatively low, long-chain FAMEs C_{24}, C_{26} and C_{28} were recombined in order to provide sufficient amounts for Δ^{14}C analysis. Purified FAMEs were transferred to tin capsules and all solvent residues were allowed to evaporate to complete dryness.

AMS Measurements on Fatty Acid Methyl Esters

Δ^{14}C analysis of the FAMEs was performed at the Max Planck Institute for Biogeochemistry, Jena (Steinhof et al., 2017), using a Mini Carbon Dating System (MICADAS, Ionplus, Dietikon, Switzerland) connected via a gas interface system to a Vario Isotope Select elemental analyzer (Elementar Analysensysteme, Langenselbold, Germany) that was used as a combustion unit (Synal et al., 2007) (**Figure 2**). The settings for the MICADAS were ensured by measuring the Oxalic acid II standard (NIST SRM 4990) to account for fractionation and standard normalization. ^{14}C background of the MICADAS was quantified by ^{14}C-free CO2 reference gas.

Results are normalized to Oxalic Acid II (National Institute of Standards and Technology) primary standard. All obtained ^{14}C values were corrected for the contribution of the methyl carbon derived from the methanol ($F^{14}C = 0.00238 \pm 0.00016$) used during the derivatization of the FAs by an isotopic mass balance equation:

$$\Delta^{14}C_{FA} = \frac{\left[(n+1)\,\Delta^{14}C_{measured}\right] - \Delta^{14}C_{MeOH}}{n}$$

where n is the number of carbon atoms in the original fatty acid. All ^{14}C data are reported in **Supplementary Table S1** as F^{14}C and conventional ^{14}C ages.

Correction for Extraneous Carbon

Because ^{14}C analysis is sensitive to contributions from extraneous carbon (C_{ex}), it is mandatory to assess the amount of C_{ex} that is added to the sample during compound isolation and subsequent processing (Santos et al., 2007; Shah and Pearson, 2007; Mollenhauer and Rethemeyer, 2009; Ziolkowski and Druffel, 2009; Hanke et al., 2017). We therefore performed extensive blank corrections based on Schwab et al. (2019b) using commercially available modern-^{14}C-content (MC) and ^{14}C- dead (DC) reference materials to monitor the modern and ^{14}C-free constituents of C_{ex}, respectively. Detailed information about blank assessment can be found in Santos et al. (2010) and Hanke et al. (2017). FAMEs $C_{16:0}$ (Sigma-Aldrich, 76,119, Δ^{14}C value of 111 ± 28‰) and phenanthrene (Sigma-Aldrich, lot MKBB7303, Δ^{14}C value of -997 ± 0.1‰) were used as modern and ^{14}C-free standards, respectively, to quantify the contamination that derived from all steps in isolation of biomarkers in the HPLC and in the determination of radiocarbon in the AMS. In addition, the new oxalic acid (NOX), graphite (Merck, 50,870) and phenanthrene standards were used to quantify the EA and AMS contamination. In our approach, contaminating carbon might be taken up during process steps such as HPLC isolation (C_{HPLC}) and during AMS sample preparation and analysis itself (C_{AMS}). Accordingly, the total contamination C_{ex} is the sum of C_{HPLC} contamination and C_{AMS} contamination.

RESULTS AND DISCUSSION

High-Pressure Liquid Chromatography Isolation and Purification

A typical chromatogram of a HPLC run and corresponding retention times of FAMEs $C_{16:0}$, $C_{18:0}$, $C_{24:0}$, $C_{26:0}$ and $C_{28:0}$ is illustrated in **Figure 3**. Using an isocratic elution with acetonitrile, short- and long-chain FAMEs were well separated

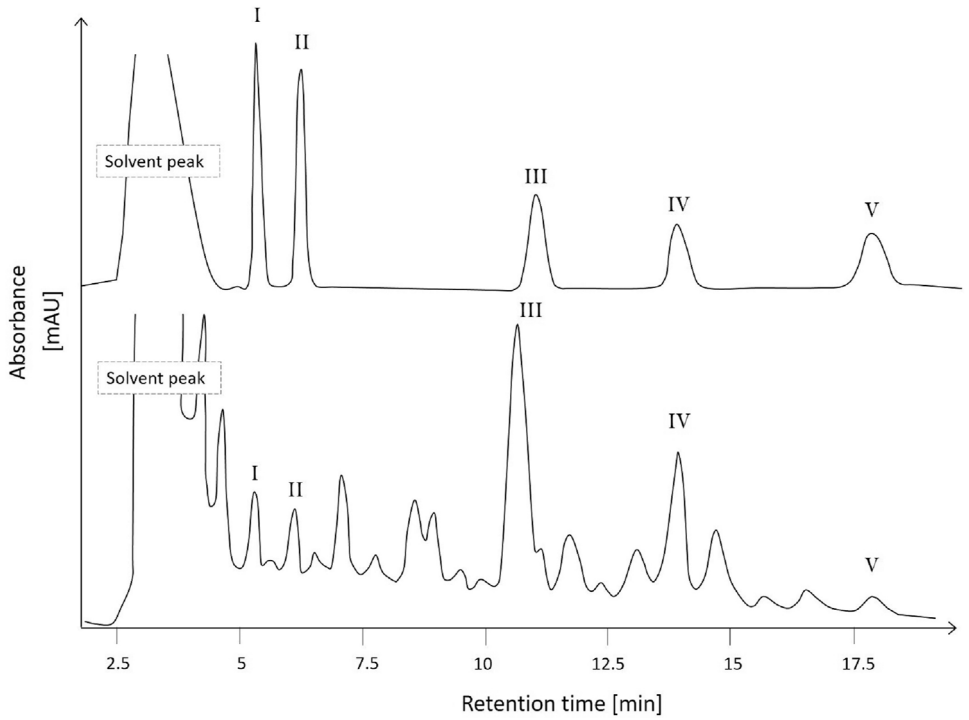

FIGURE 3 | Typical HPLC-UV/VIS chromatograms of a standard run **(upper picture)** and a sample run **(lower picture)**. Roman numbers stand for targeted saturated fatty acid methyl esters (FAMEs) with I: C16:0, II: C18:0, III: C24:0, IV: C26:0, V: C28:0.

on the reverse-phase column. Short-chain FAMEs eluted between 5 and 8 min, while long-chain FAMEs eluted between 12 and 18 min (**Figure 3**). The available carbon amounts varied between 15 and 89 μg C for the short-chain FAs and between 55 and 149 μg C for the long-chain FAs throughout the sediment record (**Supplementary Table S1**). GC-FID chromatograms of the collected fractions affirmed the purity of the isolation by HPLC (**Supplementary Figure S1**).

C_{ex} From AMS Sample Preparation and High-Pressure Liquid Chromatography Isolation

Contributions from C_{AMS} were assessed by preparing and measuring standards ranging from ^{14}C-dead to modern values (phenanthrene, graphite, oxalic acid (OX-1), FAME standards $C_{16:0}$ and $C_{26:0}$) at similar measurement conditions as the samples. The amount of carbon introduced during AMS sample preparation was 0.28 μg of MC and 0.20 μg of DC. C_{HPLC} was quantified using FAME standards $C_{16:0}$ and $C_{26:0}$ and phenanthrene. These standards were injected directly on the C8 reverse-phase column of the HPLC in different concentrations. Each injection on the HPLC was collected separately and merged to cover carbon amounts between 20 μg (1 HPLC injection) and 80 μg (10 HPLC injections) to coincide with the weight range of the carbon in the samples. The isolation via HPLC introduced DC contaminations of 0.50 ± 0.22 μg on average. The $F^{14}C$ results of our DC standards were not significantly altered by HPLC isolation, suggesting that no substantial MC contaminations were introduced by HPLC. Previous HPLC-based isolations of phospholipids resulted in highly similar contaminations of 0.57 ± 0.29 μg DC with no substantial MC being introduced (Schwab et al., 2019b). Despite the low amounts of C_{ex} that were introduced during our laboratory procedures, the $F^{14}C$ values of our sediment samples were corrected according to the DC contaminations identified through our standard measurements (**Supplementary Table S1**).

Implication of Mixed Organic Carbon Pools for Total Organic Carbon Dating

To assess the RAE on the AMS ^{14}C ages obtained from bulk sediment TOC (**Supplementary Table S2**) as well as on the ^{14}C ages obtained from FAs by CSRA (**Supplementary Table S1**), we compared these ages to the Chatvd19 varve chronology established by Kalanke et al. (2020). We found that the ^{14}C ages of TOC were substantially higher than what would be expected from the uncalibrated varve ^{14}C ages at the respective depth (**Figure 4**; and Kalanke et al. (2020), Fig. 7). Over the last ~10,000 years (based on the varve chronology), these ^{14}C ages were between ~1,000 and ~3,000 ^{14}C years older than the corresponding uncalibrated varve ^{14}C ages. The deviation increases with sediment depth, possibly related to increased input of pre-aged OC from glacial erosion material during the early Holocene. This reveals that 1) the sediments of

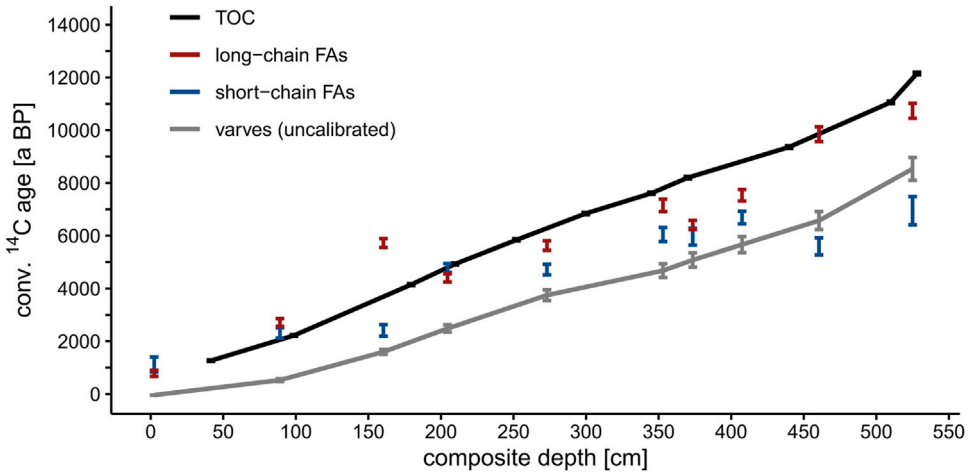

FIGURE 4 | ^{14}C ages of bulk sediment TOC as well as, short-chain and long-chain FAs obtained from the CHAT12 sediments in comparison to the uncalibrated varve ^{14}C ages reveal a temporally variable lake reservoir effect at Lake Chatyr Kol.

Lake Chatyr Kol were strongly affected by the RAE in the past and 2) the magnitude of the RAE was highly variable through time.

The CSRA of the short- and long-chain FAs yielded ^{14}C ages ranging between the TOC ^{14}C ages and the uncalibrated varve ^{14}C ages for most of the composite sediment core. The ^{14}C ages of the long-chain FAs are systematically older than those of the short-chain FAs (average ~1,430 ^{14}C years, maximum ~4,250 ^{14}C years). As the long-chain FA ^{14}C ages were closer to the TOC ^{14}C ages than the uncalibrated varve ^{14}C ages, a major source of pre-aged terrestrial OC likely contributed to the complex TOC mixture. In contrast, the ^{14}C ages of the short-chain FAs reveal a smaller offset compared to the uncalibrated varve ^{14}C ages than those of the long-chain FAs, suggesting that compound-specific sources, transport and pre-deposition aging processes control the magnitude and variability of the RAE in the Lake Chatyr Kol sediments. Long-chain FAs (>C_{24}) are generally considered to derive from terrigenous sources such as higher plant leaf waxes (McIntosh et al., 2015; Meyers, 1997; Parkes and Taylor, 1983) and can thus be utilized as tracers of terrestrial vascular plant carbon. In contrast, short-chain FAs (C_{16} and C_{18}) are, though being ubiquitous lipids, mostly ascribed to *in situ* autotrophic and heterotrophic microbes (Cranwell et al., 1987; Meyers, 1997; Tao et al., 2017). In addition, their respective transport mechanisms greatly depend on the FAs chemical properties: short-chain FAs are more water-soluble than long-chain FAs and hence can be mobilized more easily from soils and are preferentially degraded by microorganisms (Matsumoto et al., 2007). In contrast, long-chain FAs are less water-soluble and consequently more resistant to microbial degradation (Matsumoto et al., 2007; Moucawi et al., 1981). Their relative persistence and delayed transport properties, which derive from their chemical characteristics, can explain the higher ^{14}C ages of the long-chain FAs in the Lake Chatyr Kol sediment record compared to their short-chain homologues. Nevertheless, the short-chain FAs are also characterized by higher ^{14}C ages than would be expected from the varve counting at the respective depths in the composite profile.

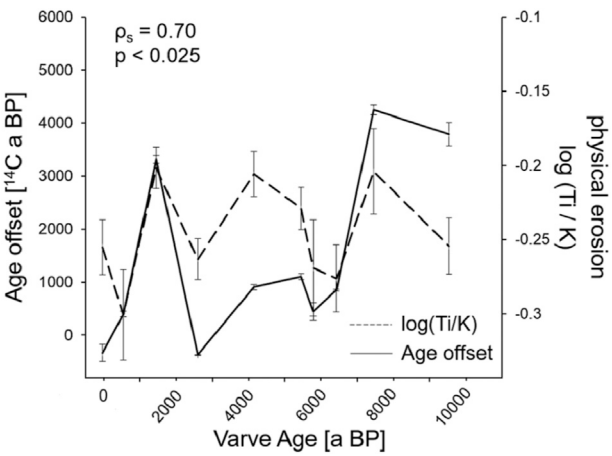

FIGURE 5 | The observed offset between the long- and short-chain FAs is highly correlated to changes in the log(Ti/K) of the sediment, indicating that mobilization of pre-aged OC from the catchment is a major determinant of RAE magnitude. Error bars on the log(Ti/K) data show the standard deviation within a 1.2-cm sediment interval across the positions where samples for CSRA were taken.

Short-chain FAs are likely influenced by the ^{14}C content of dissolved inorganic carbon (DIC) prevailing in the lake, which can, for example, be influenced by the input of surface water and/or groundwater ^{14}C (Zhou et al., 2015; Zhou et al., 2020). They could further be affected by the exchange rate between the lakes surface and atmospheric CO_2 resulting in ^{14}C depleted lake water compared to the atmosphere (Sayle et al., 2016; Zhou et al., 2020). Consequently, aquatic plants may assimilate ^{14}C-depleted DIC during photosynthesis and therefore may appear older than the deposition age. This is evidenced by the discrepancy between the aquatic macro remain-derived ^{14}C ages and the Chatvd19 varve chronology reported in Kalanke et al. (2020), **Figure 5**. Furthermore, remobilization of pre-aged terrestrial OC that

enters the lake needs to be considered as an influence on the ^{14}C ages derived from short-chain FAs (Howarth et al., 2013). While we cannot disentangle the individual effects of ^{14}C-depletion on TOC in both short- and long-chain FAs, our data indicate a common trend towards an increasing magnitude of the RAE with sediment depth. We therefore hypothesize that instead of compound-specific characteristics, the overarching temporal trend potentially resulted from system-wide shifts in OC input from the catchment.

To assess variations in the mobilization of OC from the catchment we measured the Ti/K log-ratio of the sediment (**Supplementary Figure S2**). The elements K and Ti are both confined to the detrital sediment fraction, therefore variations in the log(Ti/K) record indicate relative variations in its composition. Ti/K has previously been used as a proxy for grain-size variability in allochthonous material (Gascon Diez et al., 2017; Marshall et al., 2011) as it reflects mineralogical variations associated with size-selective transport. In general, fine-grained detrital material such as clay contains relatively high amounts of K, whereas relatively high amounts of Ti are found in coarser sediments such as coarse silt and very fine sand (Bloemsma et al., 2012; Henares et al., 2019; Rothwell and Croudace, 2015). Grain-size sediment fractions analysed by Ausín et al. (2021) showed that OC associated with the silt fraction had higher radiocarbon ages compared to clay-associated OC in various continental margin settings. The substantial pre-aging of silt-associated OC is attributed to its tendency for resuspension and prolonged translocation as silt is generally considered non-cohesive (Ausín et al., 2021; McCave et al., 1995). Conversely, the clay fraction is considered cohesive and has been found to be associated with allochthonous OC, which is less pre-aged. Therefore, variations in the log(Ti/K) ratio in our lake sediments could indicate changes in the mobilization of allochthonous material and the pre-aging of its associated OC. Increases in the inputs of highly pre-aged OC to the lake system could consequently be a major contributor to the age offset between terrestrial and aquatic biomarkers. Indeed, the age offsets between long- and short-chain FAs in the Holocene Lake Chatyr Kol sediments are positively correlated to log(Ti/K) (Spearman rank correlation coefficient $\rho_s = 0.70$, $p < 0.025$; **Figure 5**). High log(Ti/K) values are consistent with higher age offsets, suggesting that variations in sediment supply from the catchment are an important driver of the RAE magnitude at Lake Chatyr Kol. Our findings support recent global assessments of the importance of physical erosion processes for the export of carbon from the land (Galy et al., 2015) and highlight the importance of tracking their temporal variation.

CONCLUSION

The data from the Lake Chatyr Kol sediment record show that in lacustrine systems with temporally variable influx from the catchment, the magnitude of the RAE can be highly variable. Therefore, assuming a temporally constant RAE and applying a respective age correction may be misleading and can result in severely offset chronologies (e.g. Smittenberg et al., 2004; Gierga et al., 2016; Hein et al., 2020). In the case of Lake Chatyr Kol, the CSRA results quantify the discrepancies between aquatic and terrestrial biomarker ^{14}C ages to up to ~4,250 ^{14}C years and furthermore provide insights into the relationship between catchment processes and lacustrine biomarker deposition. Therefore, several factors of OC dynamics and transport mechanisms need to be considered in the study of OC cycling. Although CSRA is generally considered very time-consuming and analytically challenging, this study introduces a rapid HPLC-based method for isolating short- and long-chain FAs. With only few injections, the reported HPLC approach can provide sufficient amounts of carbon for ^{14}C analysis while minimizing the risk of contaminations at the same time. We therefore advocate for the regular implementation of compound-specific ^{14}C dating, as methodological advances give easier access to CSRA and ^{14}C dating of bulk sediment TOC is often less reliable. The data from Lake Chatyr Kol exemplify the substantial potential of compound-specific ^{14}C dating to detect temporal variations in the RAE and consequently develop more robust chronologies for lake sediment records from sparsely vegetated high-latitude and -altitude regions.

DATA AVAILABILITY STATEMENT

The raw data supporting the conclusion of this article will be made available by the authors, without undue reservation.

AUTHOR CONTRIBUTIONS

GG designed the research idea. JM and JK finalized the age model. SL conducted the field work, compiled the composite profile and selected bulk sediment and plant macro remain samples for AMS ^{14}C dating. RT provided the XRF data. NS performed laboratory analyses with the help of VS and subsequent data interpretation with support from VS and GG. NS wrote the manuscript. All authors contributed to reviewing the manuscript.

FUNDING

This study was funded by the BMBF through the research projects CADY (Central Asian Climate Dynamics, Grant No. 03G0813) and CAHOL (Central Asian Holocene Climate, Grant No. 03G0864).

ACKNOWLEDGMENTS

We thank Michael Köhler, Sylvia Pinkerneil, Robert Schedel, Denis Henning, Mirlan Daiyrov, and Roman Witt for participation in the field work and Peter Dulski for carrying out the XRF measurements. Furthermore, we thank the group of Axel Steinhof for the MICADAS radiocarbon measurements and

Achim Brauer for his project engagement. NS also acknowledges the Max Planck Society and the International Max Planck Research School for Global Biogeochemical Cycles (IMPRS-gBGC). VS acknowledges support from the European Research Council (ERC) Advanced Grant 695101 ^{14}Constraint.

SUPPLEMENTARY MATERIAL

The Supplementary Material for this article can be found online at: https://www.frontiersin.org/articles/10.3389/feart.2021.681931/full#supplementary-material

REFERENCES

Abuduwaili, J., Issanova, G., and Saparov, G. (2019). *Lakes in Kyrgyzstan, Hydrology and Limnology of Central Asia*. Singapore: Springer, 288–294.

Aizen, E. M., Aizen, V. B., Melack, J. M., Nakamura, T., and Ohta, T. (2001). Precipitation and Atmospheric Circulation Patterns at Mid-latitudes of Asia. *Int. J. Climatol.* 21 (5), 535–556. doi:10.1002/joc.626

Aizen, V., Aizen, E., Melack, J., and Dozier, J. (1997). Climatic and Hydrologic Changes in the Tien Shan, Central Asia: Journal of Climate 10, 1393–1404. doi:10.1175/1520-0442(1997)010<1393:CAHCIT>2.0.CO;2

Aizen, V. B., Aizen, E. M., and Melack, J. M. (1995). Climate, Snow Cover, Glaciers, and Runoff in the Tien Shan, Central Asia. *J. Am. Water Resour. Assoc* 31, 1113–1129. doi:10.1111/j.1752-1688.1995.tb03426.x

Appleby, P. G., and Oldfield, F. (1978). The Calculation of lead-210 Dates Assuming a Constant Rate of Supply of Unsupported 210Pb to the Sediment. *Catena* 5 (1), 1–8. doi:10.1016/S0341-8162(78)80002-2

Ausín, B., Bruni, E., Haghipour, N., Welte, C., Bernasconi, S. M., and Eglinton, T. I. (2021). Controls on the Abundance, Provenance and Age of Organic Carbon Buried in continental Margin Sediments. *Earth Planet. Sci. Lett.* 558, 116759. doi:10.1016/j.epsl.2021.116759

Bertrand, S., Araneda, A., Vargas, P., Jana, P., Fagel, N., and Urrutia, R. (2012). Using the N/C Ratio to Correct Bulk Radiocarbon Ages from lake Sediments: Insights from Chilean Patagonia. *Quat. Geochronol.* 12, 23–29. doi:10.1016/j.quageo.2012.06.003

Bloemsma, M. R., Zabel, M., Stuut, J. B. W., Tjallingii, R., Collins, J. A., and Weltje, G. J. (2012). Modelling the Joint Variability of Grain Size and Chemical Composition in Sediments. *Sediment. Geology.* 280, 135–148. doi:10.1016/j.sedgeo.2012.04.009

Bour, A. L., Walker, B. D., Broek, T. A. B., and McCarthy, M. D. (2016). Radiocarbon Analysis of Individual Amino Acids: Carbon Blank Quantification for a Small-Sample High-Pressure Liquid Chromatography Purification Method. *Anal. Chem.* 88 (7), 3521–3528. doi:10.1021/acs.analchem.5b03619

Bronk Ramsey, C. (2009). Bayesian Analysis of Radiocarbon Dates. *Radiocarbon* 51 (01), 337–360. doi:10.1017/s0033822200033865

Bronk Ramsey, C. (1995). Radiocarbon Calibration and Analysis of Stratigraphy: The OxCal Program. *Radiocarbon* 37 (2), 425–430. doi:10.1017/s0033822200030903

Cranwell, P. A., Eglinton, G., and Robinson, N. (1987). Lipids of Aquatic Organisms as Potential Contributors to Lacustrine Sediments-II. *Org. Geochem.* 11, 513–527. doi:10.1016/0146-6380(87)90007-6

Crema, E. R., and Bevan, A. (2021). Inference from Large Sets of Radiocarbon Dates: Software and Methods. *Radiocarbon* 63 (1), 23–39. doi:10.1017/RDC.2020.95

Doberschütz, S., Frenzel, P., Haberzettl, T., Kasper, T., Wang, J., Zhu, L., et al. (2014). Monsoonal Forcing of Holocene Paleoenvironmental Change on the central Tibetan Plateau Inferred Using a Sediment Record from Lake Nam Co (Xizang, China). *J. Paleolimnol* 51, 253–266. doi:10.1007/s10933-013-9702-1

Eglinton, T. I., Aluwihare, L. I., Bauer, J. E., Druffel, E. R. M., and McNichol, A. P. (1996). Gas Chromatographic Isolation of Individual Compounds from Complex Matrices for Radiocarbon Dating. *Anal. Chem.* 68 (5), 904–912. doi:10.1021/ac9508513

Eglinton, T. I., Benitez-Nelson, B. C., Pearson, A., McNichol, A. P., Bauer, J. E., and Druffel, E. R. (1997). Variability in Radiocarbon Ages of Individual Organic Compounds from marine Sediments. *Science* 277 (5327), 796–799. doi:10.1126/science.277.5327.796

Galy, V., Peucker-Ehrenbrink, B., and Eglinton, T. (2015). Global Carbon export from the Terrestrial Biosphere Controlled by Erosion. *Nature* 521, 204–207. doi:10.1038/nature14400

Gascón Díez, E., Corella, J. P., Adatte, T., Thevenon, F., and Loizeau, J.-L. (2017).High-resolution Reconstruction of the 20th century History of Trace Metals, Major Elements, and Organic Matter in Sediments in a Contaminated Area of Lake Geneva, Switzerland. *Appl. Geochem.*

Geyh, M. A., Schotterer, U., and Grosjean, M. (1998). Temporal Changes of the ^{14}C Reservoir Effect in Lakes. *Radiocarbon* 40 (2), 921–931.

Gierga, M., Hajdas, I., van Raden, U. J., Gilli, A., Wacker, L., Sturm, M., et al. (2016). Long-stored Soil Carbon Released by Prehistoric Land Use: Evidence from Compound-specific Radiocarbon Analysis on Soppensee lake Sediments. *Quat. Sci. Rev.* 144, 123–131. doi:10.1016/j.quascirev.2016.05.011

Günther, F., Thiele, A., Biskop, S., Mäusbacher, R., Haberzettl, T., Yao, T., et al. (2016). Late Quaternary Hydrological Changes at Tangra Yumco, Tibetan Plateau: a Compound-specific Isotope-Based Quantification of lake Level Changes. *J. Paleolimnol* 55 (4), 369–382. doi:10.1007/s10933-016-9887-1

Haas, M., Bliedtner, M., Borodynkin, I., Salazar, G., Szidat, S., Eglinton, T. I., et al. (2017). Radiocarbon Dating of Leaf Waxes in the Loess-Paleosol Sequence Kurtak, Central Siberia. *Radiocarbon* 59 (01), 165–176. doi:10.1017/rdc.2017.1

Hanke, U. M., Wacker, L., Haghipour, N., Schmidt, M. W. I., Eglinton, T. I., and McIntyre, C. P. (2017). Comprehensive Radiocarbon Analysis of Benzene Polycarboxylic Acids (BPCAs) Derived from Pyrogenic Carbon in Environmental Samples. *Radiocarbon* 59 (04), 1103–1116. doi:10.1017/rdc.2017.44

Hein, C. J., Usman, M., Eglinton, T. I., Haghipour, N., and Galy, V. (2020). Millennial-scale Hydroclimate Control of Tropical Soil Carbon Storage. *Nature* 581, 63–66. doi:10.1038/s41586-020-2233-9

Henares, S., Donselaar, M. E., Bloemsma, M. R., Tjallingii, R., De Wijn, B., and Weltje, G. J. (2019). Quantitative Integration of Sedimentological Core Descriptions and Petrophysical Data Using High-Resolution XRF Core Scans. *Mar. Pet. Geology.* 110, 450–462. doi:10.1016/j.marpetgeo.2019.07.034

Hou, J., D'Andrea, W. J., and Liu, Z. (2012). The Influence of 14C Reservoir Age on Interpretation of Paleolimnological Records from the Tibetan Plateau. *Quat. Sci. Rev.* 48, 67–79. doi:10.1016/j.quascirev.2012.06.008

Howarth, J. D., Fitzsimons, S. J., Jacobsen, G. E., Vandergoes, M. J., and Norris, R. J. (2013). Identifying a Reliable Target Fraction for Radiocarbon Dating Sedimentary Records from Lakes. *Quat. Geochronol.* 17, 68–80. doi:10.1016/j.quageo.2013.02.001

Hughen, K., Lehman, S., Southon, J. R., Overpeck, J. T., Marchal, O., Herring, C., et al. (2004). 14C Activity and Global Carbon Cycle Changes over the Past 50,000 Years. *Science* 303 (5655), 202–207. doi:10.1126/science.1090300

Ilyasov, S., Zabenko, O., Gaydamak, N., Kirilenko, A., Myrsaliev, N., Shevchenko, V., et al. (2013). *Climate Profile of the Kyrgyz Republic*. Bishkek, Kyrgyzstan: The State Agency for Environmental Protection and Forestry under the Government of the Kyrgyz Republic and The United Nations Development Programme, 99.

Ingalls, A. E., Ellis, E. E., Santos, G. M., McDuffee, K. E., Truxal, L., Keil, R. G., et al. (2010). HPLC Purification of Higher Plant-Dervied Lignin Phenols for Compound Specific Radiocarbon Analysis. *Anal. Chem.* 82 (21), 8931–8938. doi:10.1021/ac1016584

Ishikawa, N. F., Itahashi, Y., Blattmann, T. M., Takano, Y., Ogawa, N. O., Yamane, M., et al. (2018). Improved Method for Isolation and Purification of Underivatized Amino Acids for Radiocarbon Analysis. *Anal. Chem.* 90 (20), 12035–12041. doi:10.1021/acs.analchem.8b02693

Kalanke, J., Mingram, J., Lauterbach, S., Usubaliev, R., Tjallingii, R., and Brauer, A. (2020). Seasonal Deposition Processes and Chronology of a Varved Holocene lake Sediment Record from Chatyr Kol lake (Kyrgyz Republic). *Geochronology* 2, 133–154. doi:10.5194/gchron-2-133-2020

Koppes, M., Gillespie, A. R., Burke, R. M., Thompson, S. C., and Stone, J. (2008). Late Quaternary Glaciation in the Kyrgyz Tien Shan. *Quat. Sci. Rev.* 27 (7-8), 846–866. doi:10.1016/j.quascirev.2008.01.009

Kramer, C., and Gleixner, G. (2006). Variable Use of Plant- and Soil-Derived Carbon by Microorganisms in Agricultural Soils. *Soil Biol. Biochem.* 38 (11), 3267–3278. doi:10.1016/j.soilbio.2006.04.006

Kudo, A., Zheng, J., Koerner, R. M., Fisher, D. A., Santry, D. C., Mahara, Y., et al. (1998). Global Transport Rates of 137Cs and 239+240Pu Originating from the Nagasaki A-Bomb in 1945 as Determined from Analysis of Canadian Arctic Ice Cores. *J. Environ. Radioactivity* 40 (3), 289–298. doi:10.1016/S0265-931X(97)00023-4

Lauterbach, S., Witt, R., Plessen, B., Dulski, P., Prasad, S., Mingram, J., et al. (2014). Climatic Imprint of the Mid-latitude Westerlies in the Central Tian Shan of Kyrgyzstan and Teleconnections to North Atlantic Climate Variability during the Last 6000 Years. *The Holocene* 24 (8), 970–984. doi:10.1177/0959683614534741

Liang, E. Y., Shao, X. M., and Xu, Y. (2009). Tree-ring Evidence of Recent Abnormal Warming on the Southeast Tibetan Plateau. *Theor. Appl. Climatol* 98 (1-2), 9–18. doi:10.1007/s00704-008-0085-6

Makou, M., Eglinton, T., McIntyre, C., Montluçon, D., Antheaume, I., and Grossi(2018). Plant Wax N -Alkane and N -Alkanoic Acid Signatures Overprinted by Microbial Contributions and Old Carbon in Meromictic Lake Sediments. *Geophys. Res. Lett.* 45 (2), 1049–1057. doi:10.1002/10.1002/2017gl076211

Marshall, M. H., Lamb, H. F., Huws, D., Davies, S. J., Bates, R., Bloemendal, J., et al. (2011). Late Pleistocene and Holocene Drought Events at Lake Tana, the Source of the Blue Nile. *Glob. Planet. Change* 78 (3–4), 147–161. doi:10.1016/j.gloplacha.2011.06.004

Matsumoto, K., Kawamura, K., Uchida, M., and Shibata, Y. (2007). Radiocarbon Content and Stable Carbon Isotopic Ratios of Individual Fatty Acids in Subsurface Soil: Implication for Selective Microbial Degradation and Modification of Soil Organic Matter. *Geochem. J.* 41 (6), 483–492. doi:10.2343/geochemj.41.483

McCave, I. N., Manighetti, B., and Robinson, S. G. (1995). Sortable silt and fine Sediment Size/composition Slicing: Parameters for Palaeocurrent Speed and Palaeoceanography. *Paleoceanography* 10 (3), 593–610. doi:10.1029/94PA03039

McIntosh, H. A., McNichol, A. P., Xu, L., and Canuel, E. A. (2015). Source-age Dynamics of Estuarine Particulate Organic Matter Using Fatty Acid δ 13 C and Δ14 C Composition. *Limnol. Oceanogr.* 60 (2), 611–628. doi:10.1002/lno.10053

Meyers, P. A. (1997). Organic Geochemical Proxies of Paleoceanographic, Paleolimnologic, and Paleoclimatic Processes. *Org. Geochem.* 27 (5–6), 213–250. doi:10.1016/S0146-6380(97)00049-1

Mischke, S., Weynell, M., Zhang, C., and Wiechert, U. (2013). Spatial Variability of 14C Reservoir Effects in Tibetan Plateau Lakes. *Quat. Int.* 313-314, 147–155. doi:10.1016/j.quaint.2013.01.030

Mollenhauer, G., and Rethemeyer, J. (2009). Compound-specific Radiocarbon Analysis - Analytical Challenges and Applications. *IOP Conf. Ser. Earth Environ. Sci.* 5, 012006. doi:10.1088/1755-1307/5/1/012006

Mosello, B. (2015). The Syr Darya River Basin. *The Syr Darya River Basin, How to Deal with Climate Change?*. Berlin, Germany. Springer International Publishing, 117–162. doi:10.1007/978-3-319-15389-6_5

Moucawi, J., Fustec, E., Jambu, P., and Jacquesy, R. (1981). Decomposition of Lipids in Soils: Free and Esterified Fatty Acids, Alcohols and Ketones. *Soil Biol. Biochem.* 13 (6), 461–468. doi:10.1016/0038-0717(81)90035-3

Mügler, I., Gleixner, G., Günther, F., Mäusbacher, R., Daut, G., Schütt, B., et al. (2010). A Multi-Proxy Approach to Reconstruct Hydrological Changes and Holocene Climate Development of Nam Co, Central Tibet. *J. Paleolimnol* 43 (4), 625–648. doi:10.1007/s10933-009-9357-0

Parkes, R. J., and Taylor, J. (1983). The Relationship between Fatty Acid Distributions and Bacterial Respiratory Types in Contemporary marine Sediments. *Estuarine, Coastal Shelf Sci.* 16 (2), 173–189. doi:10.1016/0272-7714(83)90139-7

Pearson, A., McNichol, A. P., Schneider, R. J., Von Reden, K. F., and Zheng, Y. (1997). Microscale AMS 14C Measurement at NOSAMS. *Radiocarbon* 40 (01), 61–75. doi:10.1017/s0033822200017902

Pennington, W., Tutin, T. G., Cambray, R. S., and Fisher, E. M. (1973). Observations on Lake Sediments Using Fallout 137Cs as a Tracer. *Nature* 242, 324–326. doi:10.1038/242324a0

Philippsen, B. (2013). The Freshwater Reservoir Effect in Radiocarbon Dating. *Heritage Sci.* 1 (24), 24–19. doi:10.1186/2050-7445-1-24

R Core Team (2021). *R: A Language and Environment for Statistical Computing*. Vienna, Austria: R Foundation for Statistical Computing.

Reimer, P. J., Bard, E., Bayliss, A., Beck, J. W., Blackwell, P. G., Ramsey, C. B., et al. (2013). IntCal13 and Marine13 Radiocarbon Age Calibration Curves 0-50,000 Years Cal BP. *Radiocarbon* 55 (04), 1869–1887. doi:10.2458/azu_js_rc.55.16947

Robbins, J. A. (1978). "Geochemical and Geophysical Applications of Radioactive lead," in *Biogeochemistry of Lead in the Environment*. Editor J. O. Nriagu (Amsterdam: Elsevier Scientific), 285–393.

Rothwell, R. G., and Croudace, I. W. (2015). "Twenty Years of XRF Core Scanning Marine Sediments: What Do Geochemical Proxies Tell Us?," in *Micro-XRF Studies of Sediment Cores. Developments in Paleoenvironmental Research*. Editors I. W. Croudace and R. G. Rothwell (Dordrecht: Springer), Vol. 17.

Santos, G. M., Southon, J. R., Drenzek, N. J., Ziolkowski, L. A., Druffel, E. R., Xu, X., et al. (2010). Blank Assessment for Ultra-small Radiocarbon Samples: Chemical Extraction and Seperation versus AMS. *Radiocarbon.* 52 (2-3), 1322–1335. doi:10.1017/s0033822200046415

Santos, G. M., Southon, J. R., Griffin, S., Beaupre, S. R., and Druffel, E. R. M. (2007). Ultra Small-Mass AMS 14C Sample Preparation and Analyses at KCCAMS/UCI Facility. *Nucl. Instr. Methods Phys. Res. Section B: Beam Interactions Mater. Atoms* 259 (1), 293–302. doi:10.1016/j.nimb.2007.01.172

Sayle, K. L., Hamilton, W. D., Gestsdóttir, H., and Cook, G. T. (2016). Modelling Lake Mývatn's Freshwater Reservoir Effect: Utilisation of the Statistical Program FRUITS to Assist in the Re-interpretation of Radiocarbon Dates from a Cemetery at Hofstaðir, north-east Iceland. *Quat. Geochronol.* 36, 1–11. doi:10.1016/j.quageo.2016.07.001

Schwab, F., Nowak, M. E., Elder, C. D., Trumbore, S. E., Xu, X., Gleixner, G., et al. (2019a). 14 C-Free Carbon Is a Major Contributor to Cellular Biomass in Geochemically Distinct Groundwater of Shallow Sedimentary Bedrock Aquifers. *Water Resour. Res.* 55 (3), 2104–2121. doi:10.1029/2017WR022067

Schwab, F., Nowak, M. E., Trumbore, S. E., Xu, X., Gleixner, G., Muhr, J., et al. (2019b). Isolation of Individual Saturated Fatty Acid Methyl Esters Derived from Groundwater Phospholipids by Preparative High-Pressure Liquid Chromatography for Compound-Specific Radiocarbon Analyses. *Water Resour. Res.* 55 (11), 2521–2531. doi:10.1029/2018WR024076

Shah, S. R., and Pearson, A. (2007). Ultra-Microscale (5-25 μg C) Analysis of Individual Lipids by 14C AMS: Assessment and Correction for Sample Processing Blanks. *Radiocarbon* 49 (1), 69–82. doi:10.2458/azu_js_rc.49.290010.1017/s0033822200041904

Sheppard, P. R., Tarasov, P. E., Graumlich, L. J., Heussner, K.-U., Wagner, M., sterle, H., et al. (2004). Annual Precipitation since 515 BC Reconstructed from Living and Fossil Juniper Growth of Northeastern Qinghai Province, China. *Clim. Dyn.* 23 (7-8), 869–881. doi:10.1007/s00382-004-0473-2

Shnitnikov, A. V., Livja, A. A., Berdovskaya, G. N., and Sevastianov, D. V. (1978). Paleolimnology of Chatyrkel Lake (Tien-Shan). *Polskie Archiwum Hydrobiologii* 25, 383–390.

Sidorov, D. A. (2012). Two New Species of Freshwater Amphipods (Crustacea: Gammaridae) from Central Asia, with Comments on the Unusual Upper Lip Morphology. *Zootaxa* 3317, 1–24. doi:10.11646/zootaxa.3317.1.1

Smittenberg, R. H., Hopmans, E. C., Schouten, S., Hayes, J. M., Eglinton, T. I., and Sinninghe Damsté, J. S. (2004). Compound-specific Radiocarbon Dating of the Varved Holocene Sedimentary Record of Saanich Inlet, Canada. *Paleoceanography* 19 (2), a–n. doi:10.1029/2003pa000927

Soulet, G. (2015). Methods and Codes for Reservoir-Atmosphere 14 C Age Offset Calculations. *Quat. Geochronol.* 29, 97–103. doi:10.1016/j.quageo.2015.05.023

Soulet, G., Skinner, L. C., Beaupré, S. R., and Galy(2016). A Note on Reporting of Reservoir 14C Disequilibria and Age Offsets. *Radiocarbon* 58 (1), 205–211. doi:10.1017/RDC.2015.22

Steinhof, A., Altenburg, M., and Machts, H. (2017). Sample Preparation at the Jena 14C Laboratory. *Radiocarbon* 59, 815–830. doi:10.1017/RDC.2017.50

Synal, H.-A., Stocker, M., and Suter, M. (2007). MICADAS: A New Compact Radiocarbon AMS System. *Nucl. Instr. Methods Phys. Res. Section B: Beam Interactions Mater. Atoms* 259 (1), 7–13. doi:10.1016/j.nimb.2007.01.138

Taft, J. B., Phillippe, L. R., Dietrich, C. H., and Robertson, K. R. (2011). Grassland Composition, Structure, and Diversity Patterns along Major Environmental

Gradients in the Central Tien Shan. *Plant Ecol.* 212 (8), 1349–1361. doi:10.1007/s11258-011-9911-5

Tao, S., Yin, X., Jiao, L., Zhao, S., and Chen, L. (2017). Temporal Variability of Source-specific Solvent-Extractable Organic Compounds in Coastal Aerosols over Xiamen, China. *Atmosphere* 8 (33)–33. doi:10.3390/atmos8020033

Thompson, L. G., Mosley-Thompson, E., Davis, M. E., Mashiotta, T. A., Henderson, K. A., Lin, P.-N., et al. (2006a). Ice Core Evidence for Asynchronous Glaciation on the Tibetan Plateau. *Quat. Int.* 154-155, 3–10. doi:10.1016/j.quaint.2006.02.001

Thompson, L. G., Tandong, Y., Davis, M. E., Mosley-Thompson, E., Mashiotta, T. A., Lin, P.-N., et al. (2006b). Holocene Climate Variability Archived in the Puruogangri Ice Cap on the central Tibetan Plateau. *Ann. Glaciol.* 43, 61–69. doi:10.3189/172756406781812357

Thompson, L. G., Yao, T., Davis, M., Henderson, K. A., Mosley-Thompson, E., Lin, P.-N., et al. (1997). Tropical Climate Instability: The Last Glacial Cycle from a Qinghai-Tibetan Ice Core. *Science* 276 (5320), 1821–1825. doi:10.1126/science.276.5320.1821

Thorpe, A., van Anrooy, R., Niyazov, B. N., Sarieva, M. K., Valbo-Jørgensen, J., and Millar, A. M. (2009). The Collapse of the Fisheries Sector in Kyrgyzstan: An Analysis of its Roots and its Prospects for Revival. *Communist Post-Communist Stud.* 42 (1), 141–163. doi:10.1016/j.postcomstud.2009.02.007

Weltje, G. J., and Tjallingii, R. (2008). Calibration of XRF Core Scanners for Quantitative Geochemical Logging of Sediment Cores: Theory and Application. *Earth Planet. Sci. Lett.* 274 (3–4), 423–438. doi:10.1016/j.epsl.2008.07.054

Wright, S. M., Howard, B. J., Strand, P., Nylén, T., and Sickel, M. A. K. (1999). Prediction of 137Cs Deposition from Atmospheric Nuclear Weapons Tests within the Arctic. *Environ. Pollut.* 104 (1), 131–143. doi:10.1016/S0269-7491(98)00140-7

Yang, B., Qin, C., Wang, J., He, M., Melvin, T. M., Osborn, T. J., et al. (2014). A 3,500-year Tree-Ring Record of Annual Precipitation on the Northeastern Tibetan Plateau. *Proc. Natl. Acad. Sci.* 111 (8), 2903–2908. doi:10.1073/pnas.1319238111

Yao, T., Thompson, L. G., Mosley-Thompson, E., Zhihong, Y., Xingping, Z., and Lin, P.-N. (1996). Climatological Significance of δ18O in north Tibetan Ice Cores. *J. Geophys. Res.* 101 (D23), 29531–29537. doi:10.1029/96jd02683

Yokoyama, Y., Koizumi, M., Matsuzaki, H., Miyairi, Y., and Ohkouchi, N. (2010). Developing Ultra Small-Scale Radiocarbon Sample Measurement at the University of Tokyo, 52. *Radiocarbon*, 310–318. doi:10.1017/s0033822200045355

Zhang, H., Wang, R., and Xiao, W. (2017). Paleoenvironmental Implications of Holocene Long-Chain *N*-Alkanes on the Northern Bering Sea Slope. *Acta Oceanol. Sin.* 36 (8), 137–145. doi:10.1007/s13131-017-1032-0

Zhang, J., Ma, X., Qiang, M., Huang, X., Li, S., Guo, X., et al. (2016). Developing Inorganic Carbon-Based Radiocarbon Chronologies for Holocene lake Sediments in Arid NW China. *Quat. Sci. Rev.* 144, 66–82. doi:10.1016/j.quascirev.2016.05.034

Zhou, A., He, Y., Wu, D., Zhang, X., Zhang, C., Liu, Z., et al. (2015). Changes in the Radiocarbon Reservoir Age in Lake Xingyun, Southwestern China during the Holocene. *PLoS One* 10 (3), e0121532. doi:10.1371/journal.pone.0121532

Zhou, K. e., Xu, H., Lan, J., Yan, D., Sheng, E., Yu, K., et al. (2020). Variable Late Holocene 14C Reservoir Ages in Lake Bosten, Northwestern China. *Front. Earth Sci.* 7–328. doi:10.3389/feart.2019.00328

Ziolkowski, L. A., and Druffel, E. R. M. (2009). Quantification of Extraneous Carbon during Compound Specific Radiocarbon Analysis of Black Carbon. *Anal. Chem.* 81 (24), 10156–10161. doi:10.1021/ac901922s

Conflict of Interest: The authors declare that the research was conducted in the absence of any commercial or financial relationships that could be construed as a potential conflict of interest.